



UNIVERSITÀ DI PARMA

ARCHIVIO DELLA RICERCA

University of Parma Research Repository

Coupling excavator hydraulic system and internal combustion engine models for the real-time simulation

This is the peer reviewed version of the following article:

Original

Coupling excavator hydraulic system and internal combustion engine models for the real-time simulation / Casoli, Paolo; Gambarotta, Agostino; Pompini, Nicola; Ricco', Luca. - In: CONTROL ENGINEERING PRACTICE. - ISSN 0967-0661. - 41(2015), pp. 26-37. [10.1016/j.conengprac.2015.04.003]

Availability:

This version is available at: 11381/2789171 since: 2021-11-05T15:25:54Z

Publisher:

Elsevier Ltd

Published

DOI:10.1016/j.conengprac.2015.04.003

Terms of use:

openAccess

Anyone can freely access the full text of works made available as "Open Access". Works made available

Publisher copyright

(Article begins on next page)

Coupling excavator hydraulic system and internal combustion engine models for the Real-Time simulation

Paolo Casoli^{1,*}, Agostino Gambarotta¹, Nicola Pompini¹ and Luca Riccò¹

¹ *Industrial Engineering Department, University of Parma Italy, Parco Area delle Scienze 181/A, 43124 Parma (PR)*

ITALY

* Corresponding Author: e-Mail: paolo.casoli@unipr.it

Tel.: +39-0521-905868; Fax: +39-0521-905705.

Abstract: Rising energy costs and emissions restrictions force manufacturers to exploit new techniques to reduce fuel consumption and pollutant production. Many solutions have been proposed for off-road vehicles, mainly based on reduction of hydraulic losses, better control strategies and introduction of hybrid architectures. In these applications the optimization of the matching between hydraulic system and thermal engine is a major concern to improve system overall efficiency. The work presented in the paper is focused on the development of a method for the simulation of typical mobile machinery where hydraulic systems are powered by internal combustion engines; the proposed co-simulation approach can be useful in the development cycle of this machinery.

Keywords: “Control-oriented” Modelling; Hydraulic Excavator; Variable Displacement Pump; Co-simulation of complex systems; Modelling.

1. Introduction

Fuel consumption and pollutant emissions are and will continue to be the driving forces in the improvement of vehicles, i.e., cars, trucks as well as earth movers and construction machines. These aspects are amplified by more stringent emissions regulations that nowadays are going to impact also off-highway vehicles development. Many solutions have been proposed recently to reduce the energy consumption of off-road vehicles, mainly based on reduction of hydraulic losses, better control strategies of hydraulic systems and the introduction of hybrid architectures [1, 2, 3]. For off-road vehicles, the energy storage systems of an hybrid architectures could be electric batteries or hydraulic accumulators. If electric batteries have high energy density, hydraulic accumulators show higher power density and energy conversion efficiency that are needed to effectively recover mechanical energy [4, 5, 6]. A number of proposals can be found in the literature for the development of Hydraulic Hybrid Systems (HHS), as reported in [6, 7, 8].

35 In the mentioned applications, the optimization of the matching between hydraulic system and
36 internal combustion engine is one of the major concerns for the improvement of system overall
37 efficiency and the reduction of fuel consumption. Virtual design based on mathematical models is a
38 widely used option to match system components making the best use of their operating characteristics.
39 Generally speaking, this is the case when dealing with complex systems, where the ability to simulate
40 interactions between system components in real operating conditions is a primary concern for the
41 optimization of system layout and management. When dealing with the simulation of hydraulic circuits
42 and primary engines several problems arise, and this is probably the reason why up to now in most of
43 the proposed models of hydraulic off-road vehicles thermal engine is not considered or otherwise is
44 modelled following map-based approaches (several examples can be found in [3, 6, 7, 8, 9, 10, 11,
45 12]), with very few and recent exceptions [13].

46 Mathematical models have been used within several steps of the design process in systems
47 engineering, but with the continuing increase of computers power and the improvement of
48 computational methods, simulation tools are currently used in every phase of the development cycle
49 (the so-called V-cycle [14]). Usually, models with different levels of detail – and therefore with
50 different complexity – are used at each stage of the development process. In the concept stage, very
51 fast, low fidelity models are required for rapid architecture and concept analysis, while coming to an
52 exhaustive design and optimization of components and sub-systems, detailed 1-D to 3-D models are
53 used. Faster, lower fidelity models are employed for the system integration phase, and for the
54 development and testing of control systems (i.e., ECU, control strategies, etc.) through XiL (MiL, SiL
55 and HiL) tools.

56 As a matter of fact, modelling tasks carried out throughout the development cycle involve very
57 often the use of disparate simulation tools, each committed to a specific sub-system (e.g., AMESim[®]
58 for the hydraulic system, GT-Power[®], Boost[®] or Simulink[®] for the engine, in the case of an HHS or a
59 hydraulic excavator). Even if a single simulation tool may be considered within all stages of the
60 development process, actually this approach seems to require significant efforts in terms of costs and
61 time.

62 The work presented in this paper is focused on the development of methods and techniques for
63 mathematical simulation of typical mobile machinery where hydraulic systems are powered by internal
64 combustion engines (ICEs).

65 By coupling models of a Diesel engine and the hydraulic circuit of an excavator by carefully
66 handling causality, I/O parameters and co-simulation issues, a comprehensive mathematical model was
67 set up and used to simulate steady and transient behaviour of the system. Different integration time
68 steps were defined for the two sub-models taking account of their differing numerical “stiffness”, thus
69 allowing to run the comprehensive model faster than real time.

70 A potential of this approach is the ability to develop a comprehensive control strategy for the whole
71 system, with the possibility to maximize performance and reduce fuel consumption in relation to the
72 specific tasks for the system itself was developed; rather than considering the overall system as the
73 sum of components, whose control strategies are optimized in reference to the execution of generic
74 tasks, the general control strategy can be developed to maximize the performance of the individual
75 components in the specific configuration adopted. The proposed models allow for the simulation of the
76 whole system taking account of non-linear and dynamic behaviour of its components still running in
77 Real-Time. Thanks to this, these models can be used within the design process both to define the

78 system layout and to design and test related control strategies (since they can be embedded in XiL
79 systems).

80 The engine model has been built in Simulink[®] following a “crank-angle” 0D, lumped-parameter
81 approach and allows to take account of non-linearities and low-order dynamics typical of Diesel
82 engines[25, 35]. The model of the hydraulic system was set up in AMESim[®] coupling the models of
83 all involved components (axial piston pump, flow compensators, valves, actuators, etc.) to replicate the
84 non-linear behaviour of the system with the typical fast dynamic. Kinematics of the system (e.g., arms,
85 boom, bucket, etc.) were simulated using the proper AMESim[®] libraries [15, 18]. The developed
86 models were coupled to co-simulate the behaviour of an excavator and the comprehensive model was
87 validated comparing several calculated output with the first experimental data gathered on a real
88 machine.

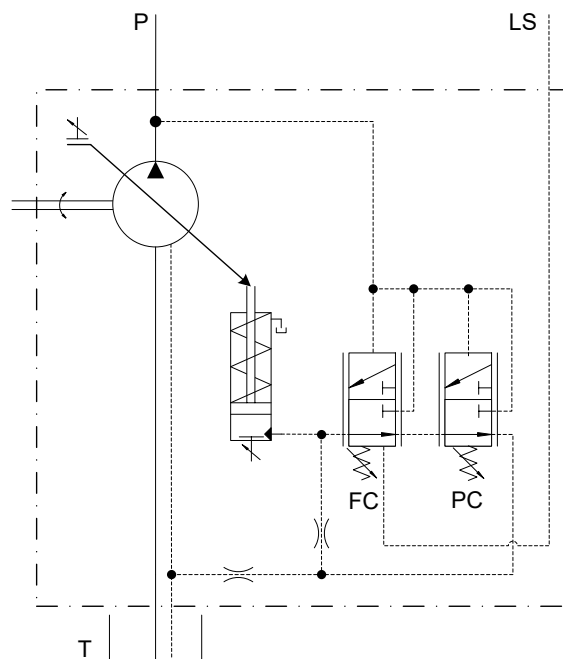
89 Results reported in the paper show to what extent the proposed co-simulation approach, based on
90 dynamic model for both the hydraulic system and the internal combustion engine, could be useful in
91 the control strategy development phase for hydraulic systems powered by Diesel engines.

92 2. Modelling of Hydraulic System

93 The hydraulic system considered is based on a typical circuit of an excavator composed of a
94 variable displacement axial piston pump with flow and pressure compensators, flow control valves and
95 hydraulic actuators as described in [18]. Kinematics of the system (e.g., arms, boom, bucket, etc.) will
96 be taken into account in the next future.

97 2.1 Variable displacement axial piston pump model

98 The pump considered in the paper is a variable displacement axial piston pump, fig. 1. The
99 comprehensive pump model includes three sub-models: the pressure compensator (PC), the flow
100 compensator (FC) and the flow generator model.



101
102

Fig.1. Pump ISO scheme

103 2.1.1 Pressure and flow compensators models.

104 The main purpose of the pressure compensator (PC) is to limit maximum value of system pressure
 105 (P line) when it is greater than a defined relief setting pressure. When this situation occurs the PC
 106 causes a rotation of the swash plate, reducing the flow rate and avoiding further increases of the system
 107 pressure. The task of the flow compensator (FC) is to offset pump displacement for a defined preload
 108 value by controlling the swash plate angle. As a common practice, a “load-sensing” pump is designed
 109 to keep a constant pressure drop across a controlling orifice in order to regulate fluid mass flow rate. In
 110 order to avoid wasting energy, the FC adjusts the pump displacement until the pump outlet pressure is
 111 greater than the load pressure of a defined quantity. The model used in this research was already
 112 presented in [15], in this work has been used a slightly simplified version of the original model where
 113 small redundant chambers and leakages, having limited effects on the pump dynamic behaviour,
 114 according to the Activity Index criteria [39, 40]. The corresponding volume increase of the remaining
 115 chambers had a positive effect to reduce numerical stiffness of the resulting model, according with
 116 Eq.(4) which clearly shows that hydraulic components have a considerably small time constant, due to
 117 the fact that even low flow rates induce high variations in chambers pressure (since mineral oils have
 118 high bulk modulus, $\beta \sim 17000$ bar).

119 2.1.2 Flow generator model

120 Several examples of pump modelling have been reported in literature [21,22, 23], but they are more
 121 suitable for internal pump’s components optimization rather than for modelling the behaviour of a
 122 pump working in complex systems. In this paper, the approach followed for the modelling is that of
 123 considering the pump as a simple flow generator for which the volumetric flow rate is calculated from
 124 the rotational speed and the pump instantaneous displacement, geometrically related to the swash plate
 125 angular position:

$$126 \quad \dot{V}_{th} = V_d(\alpha) n \quad (1)$$

127 where \dot{V}_{th} is the theoretical volumetric flow rate, α is the swash plate angular position, V_d the pump
 128 displacement, and n is the shaft rotational speed.

129 A black box model, based on experimental data, was adopted for the evaluation of the barrel torque,
 130 being the flow characteristic of the pump correlated to the equilibrium of the swash plate.

131 This was achieved by measuring the pressure in the pump actuator (which controls the
 132 corresponding actuator torque) for given values of pump outlet pressure and swash plate angular
 133 positions, and keeping the rotational speed fixed. A correlation between the pressure in the pump
 134 actuator and pump outlet pressure was consequently identified. The authors experimentally found a
 135 linear correlation between the control piston pressure and the system pressure, as already reported in
 136 [15].

137 Hydro-mechanical and volumetric efficiencies have been evaluated experimentally [24] and a
 138 correlation between η_{hm} , η_v and rotational speed, delivery pressure and swash plate displacement was
 139 identified. The real flow outlet is thereby calculated as:

$$140 \quad \dot{V} = \eta_v(p_{sys}, n, \alpha) \cdot \dot{V}_{th} \quad (2)$$

141 and the torque required at the shaft is:

142

$$T = \frac{\Delta p \cdot V_d(\alpha)}{2\pi} \cdot \frac{1}{\eta_{hm}(p_{sys}, n, \alpha)} \quad (3)$$

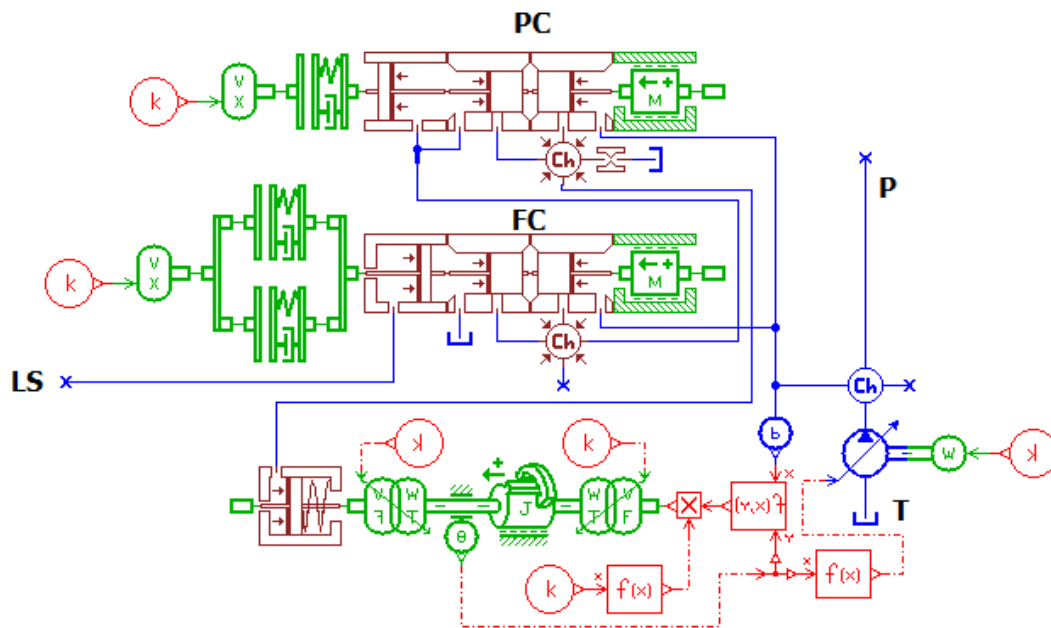
143

Where p_{sys} is the pump outlet pressure; Δp is the pressure increment through the pump.

144

The pump model was developed in AMESim[®] environment. Fig. 2 reports the sketch of the model.

145



146

147

Fig.2. AMESim[®] sketch of the pump model

148

149 2.2 Directional Valve Model

150

The considered excavator is equipped with a load sensing flow sharing valve block (Walvoil[®] DPX series). The valve section ISO scheme is reported in fig.3. The main tasks of the valve block are to govern the outlet flow rate through each single control section to the corresponding actuator, to extrapolate the LS pressure and to keep a constant pressure drop across the main spool metering area providing the flow sharing operation condition when required.

151

152

153

154

155

Usually, during a digging cycle, when the front excavation tool are operated, at least three valve sections are used at the same time, and the pump may work in flow saturation conditions (i.e., the pumps flow rate is lower than the flow required by the system to keep the required pressure across the metering areas); if this situation occurs, the load sensing flow sharing valve block still allows the operator to control safely the system, but with the excavation tool components velocities reduced. The valve's pressure compensator maintains a constant pressure drop across the spool metering area, so the result is a flow to the working port that still depends only on the spool position.

156

157

158

159

160

161

162

Each single valve section was modelled as a white box model and validated by comparison with experimental results as reported in [18].

163

164

The valve mathematical model is based on the interaction between a fluid-dynamic model (FDM) and a mechanical-geometrical model (MGM). The FDM allows the evaluation of pressures inside each control volume and the corresponding flow rates between adjacent volumes, while the MGM calculates the dynamic equilibrium of the spools estimating its positions and the corresponding orifices flow areas. Both the FDM and the MGM are based on a lumped parameter approach. In order to apply

165

166

167

168

169 the FDM and the MGM to the valve, the control volumes considered are reported in figs. 4, 5. Pressure
 170 distribution inside each control volume is assumed uniform and varying with time with a derivative
 171 that can be obtained combining continuity equation and state equation of the fluid:

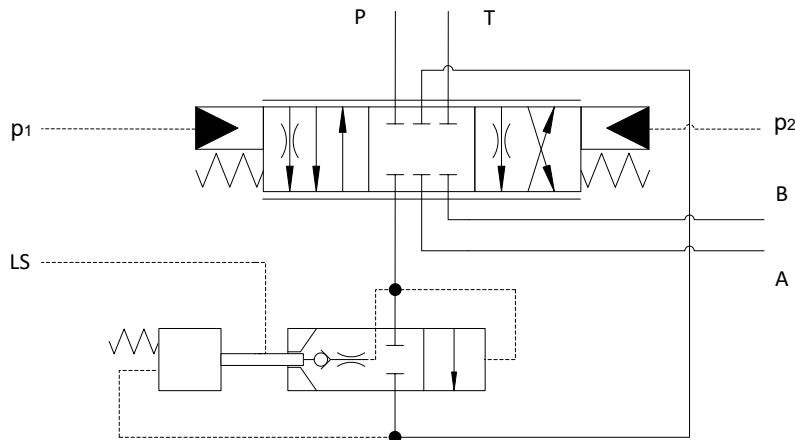
$$\frac{dp_i}{dt} = \frac{\beta}{\rho_i V_i(x)} \left(\sum \dot{m} - \rho_i \frac{dV_i(x)}{dt} \right) \quad (4)$$

173 where for the i^{th} control volume p is the absolute pressure, β is the bulk modulus, \dot{m} is the mass flow
 174 rate, ρ is the fluid density and $V(x)$ is the volume, x is the instantaneous position of the spool. Constant
 175 fluid temperature is assumed. Fluid density is evaluated as a function of pressure as described in [19,
 176 20]. The summation in eq.(4) represents the net mass flow rate entering or leaving a volume, obtained
 177 considering the contribution of all orifices connected with the considered volume. Mass flow rate
 178 through the orifices is calculated using the generalized Bernoulli's equation in quasi-steady flow
 179 conditions:

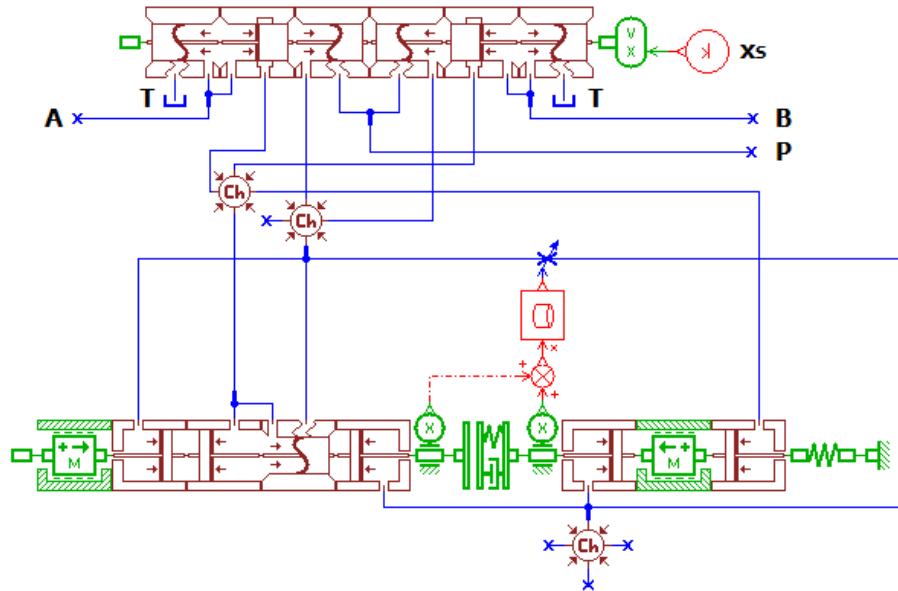
$$\dot{m} = \rho C_d A(x) \sqrt{\frac{2 |\Delta p|}{\rho}} \quad (5)$$

182 where C_d is the discharge coefficient and $A(x)$ is the flow area. A proper saturated value for the
 183 discharge coefficient of each connection was defined on the basis of experimental data or using values
 184 reported in literature [19]. Thereafter the instantaneous value of the discharge coefficient is evaluated
 185 as a function of Reynolds number to account for partially developed or fully turbulent conditions.
 186 Annular leakages past spool bodies were neglected.

187 The MGM calculates the instantaneous position and velocity of the spool from Newton's second
 188 law estimating forces acting on the spool (i.e., hydrostatic forces, spring force, friction forces,
 189 hydrodynamic forces). Static and dynamic friction forces are evaluated by use of the Karnopp friction
 190 model and considering the Stribeck effect, static and dynamic friction coefficients are assumed
 191 constant, while hydrodynamic forces are neglected.



193 **Fig.3. ISO scheme of the valve section.**
 194
 195



202
203 **Fig.6.** AMESim[®] sketch of the valve model
204

205 The valve's model was realized using the AMESim[®] Hydraulic and Mechanical library, fig.6.
206

207 **3. Modelling of the Diesel engine: methods and used approach.**

208 Several mathematical models are proposed in the open literature for the fast simulation Internal
209 Combustion Engines [25, 26]. In the development of any comprehensive engine model, simplifications
210 and approximations have to be properly introduced in order to simulate the real behaviour of the whole
211 system as a consequence of the behaviour of its components. When “Real-Time” models are required,
212 physical –and chemical– principles (generally based on conservation laws) have to be combined with
213 empirical descriptions of processes and components taking account of relevant aspects and avoiding a
214 detailed description of the others [25, 26].

215 Mean Value Models (MVMs) for the simulation of engines transients can be developed through a
216 proper alternation of Filling and Emptying (F&E) and Quasi-Steady Flow (QSF) methods [27, 28], that
217 allows taking account of low frequency processes which dominate engine behaviour. The use of F&E
218 and QSF methods in the development of 0D, lumped parameters MVMs can be structured following
219 specific criteria in order to avoid numerical problems in the simulation [29]. System components can
220 be classified as *volume components* or *capacitances*, modelled through the use of state-space
221 representations and *non-volume components* or *resistances*, modelled through algebraic equations. The
222 dynamic behaviour of the system results from the interactions between capacitances and resistances.

223 The simulation of in-cylinder processes introduces well-known difficulties, especially for Diesel
224 engines, where combustion is highly non-homogeneous. When dealing with the simulation of “cycle-
225 to-cycle” phenomena (typically intake and exhaust flows and combustion process) F&E and QSF
226 methods can still be used, but more complex models usually result, whose equations have to be
227 integrated on a crank angle base. Calculation time is usually a challenge in this case, since the
228 estimation of in-cylinder pressure and temperature histories requires more detailed approaches than
229 those used for black-box models [25, 30]. The complexity of chemical and physical processes
230 occurring in the cylinder cannot be described in detail: for fast applications simplified 0D single-zone

231 models [26, 27, 28] seem still the best option. In-cylinder processes can be simulated on a crank-angle
232 base following a F&E approach joined with a QSF technique for gas flows through valves by applying
233 the energy and mass conservation equations to a gas mixture which is considered homogeneous within
234 the cylinder (“single-zone” models). Similar models have been proposed for control-oriented
235 applications [27, 32] and used in several “crank-angle” commercial tools.

236 Within this scenario, a “crank-angle” model of a four-cylinder turbocharged Diesel engine based on
237 a single-zone scheme has been developed by the authors, and integrated within the previously
238 developed original library [17, 32, 33].

239 3.1. The simulation library for the development of I.C. Engines Mean Value Models.

240 The simulation library built up by the authors in the last decade has been conceived to create “Real-
241 Time” Mean Value Models (MVMs) of automotive engines. Based on F&E and QSF methods, and
242 developed within MATLAB[®]/Simulink[®] environment to improve portability and flexibility, the library
243 has been organised in a hierarchical structure so that sub-model blocks can be found, picked up and
244 assembled following the desired system layout. Dedicated procedures have been defined for the
245 identification of each block [34].

246 Intake and exhaust system components were modelled as volume components (i.e., capacitances)
247 through a F&E approach (e.g., manifolds), or as non-volume components (i.e., resistances) with a QSF
248 methodology (e.g., valves, compressors, turbines, etc.) [32, 33]. Processes which take place in the
249 cylinder have been modelled through a F&E method based on mass and energy conservation equations
250 applied following a single-zone approach to an open thermodynamic system in the well-known form of
251 mass and energy conservation equations, where the working fluid is assumed to be a mixture of ideal
252 gases.

253 Combustion contribution to energy conservation equation has been estimated from Watson’s
254 formulation of fuel burn fraction FB [27, 28]:

$$255 \quad FB(\theta) = \beta \cdot f_p(\theta) + (1 - \beta) \cdot f_d(\theta) \quad (6)$$

256 The fuel burn rate, function of the crank angle θ , is composed of two terms, f_p and f_d , representing
257 the pre-mixed and diffusive phases of the combustion. The shape of these two curves, which depends
258 on engine operating condition (e.g. engine shaft speed) is reported in literature [27, 28].

259 The coefficient β in eq. (11), the so-called “phase proportionality factor”, is evaluated as:

$$260 \quad \beta = 1 - \frac{a \cdot \phi^b}{\tau_{id}^c} \quad (7)$$

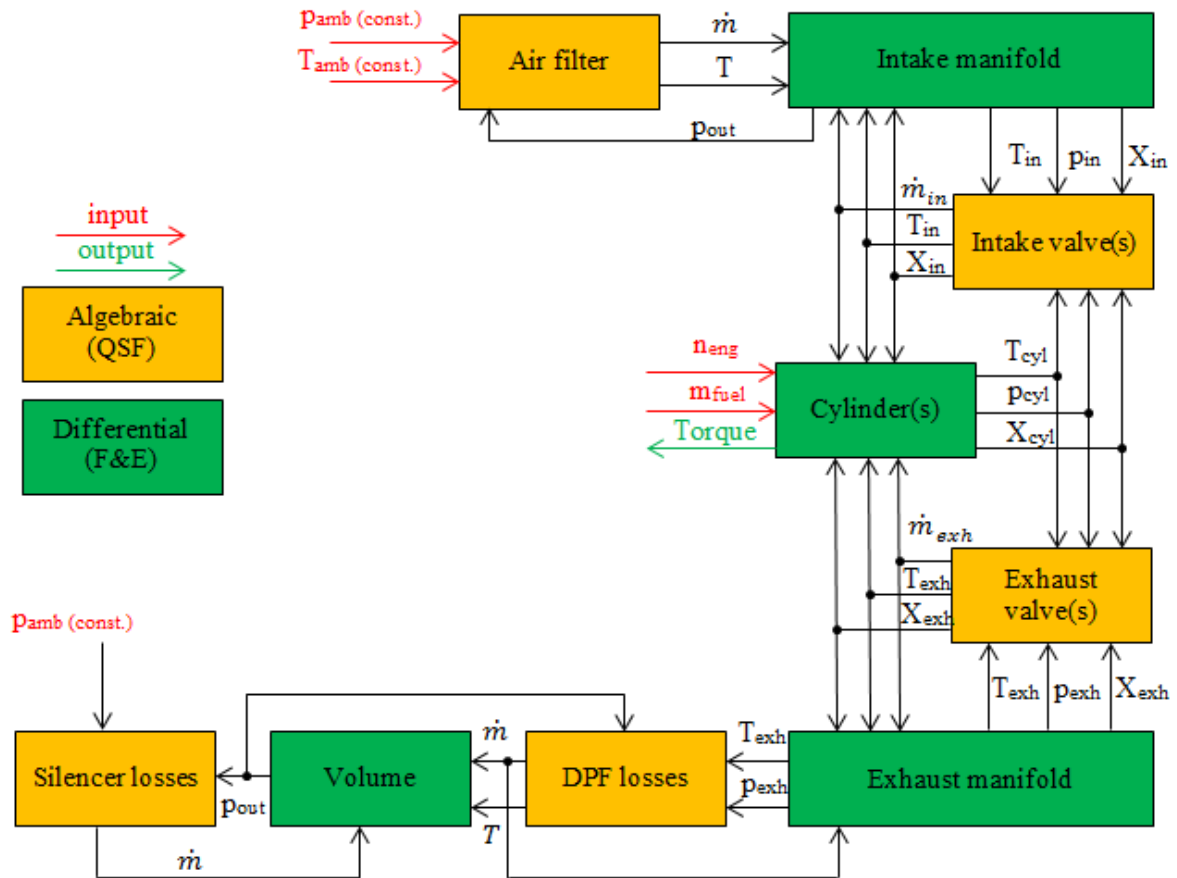
261 where ϕ is the overall fuel air ratio and τ the ignition delay, evaluated through Hardenberg and Hase
262 correlation [29]). Coefficients a , b , and c are estimated from experimental data.

263 In-cylinder equations are integrated on a crank angle base instead than time, with an angle step of 1
264 deg to avoid numerical problems. As the corresponding time step to 1 deg angle step would be too
265 little to perform fast simulations ($\sim 86 \mu s$ at 2000 r/min), the whole model uses an higher sample time,
266 1 ms, and in-cylinders equations are iteratively integrated n-times during a single time step in order to
267 obtain the required crank angle resolution. During the iterative integration, boundary conditions for the
268 in-cylinder process (e.g. engine speed, manifold pressure) are assumed to stay constant, while the

269 resulting output from the integration (e.g mass flow rates to the manifolds) are properly averaged in
 270 order to ensure mass and energy conservation [17].

271 Piston and crank inertial effect on shaft dynamics are neglected, accounting only for the slow
 272 dynamics on the mechanical part of the model.

273 Figure 7 depicts a causality diagram for the ICE, obtained by assembling the components contained
 274 in the library by the authors.



275
 276
 277

Fig.7. Causality scheme for the four-cylinder naturally aspirated Diesel engine.

278 3.2. Engine model calibration

279 The application considered in the present work equips a four cylinder direct injection, naturally
 280 aspirated, midsize Diesel engine, developed by Yanmar® (Tab.1.). The engine is equipped with an
 281 electric governor that controls the mass of injected fuel to reduce the error between measured and
 282 desired engine rotational speed. In Figs. 8 and 9 engine power output, brake torque, and BSFC
 283 characteristic curves given by Yanmar are reported.

284

Tab.1. Engine characteristics parameters

Type	four-strokes, inline, water cooled, Diesel
No. of cylinders – Bore x Stroke [mm]	4 – 98 x 110
Combustion system	direct injection
Compression ratio	18.5
Displacement [cm ³]	3319
Rated output [kW] @ 2200 r/min	46.3
Specific fuel consumption [g/kWh] @ 2200 r/min	240
Max Torque [Nm] @ 1400 r/min	228
Fuel injection timing [deg BTDC] @ 2200 r/min	13

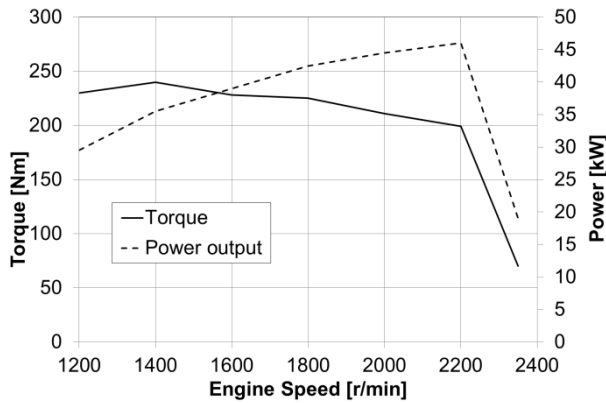


Fig.8. Engine power and torque characteristics.

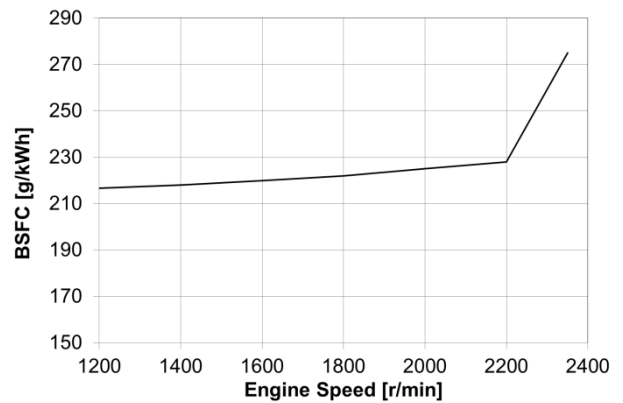


Fig.9. BSFC characteristics.

289 Input parameters of the overall engine model are ambient temperature and pressure (assumed as
290 constants), rotational speed and injected fuel mass. The model allows the evaluation of every operating
291 and state parameter (e.g., power output, temperature and composition of exhaust gases, bmep, etc.). As
292 shown in fig.10, the engine controller adjusts the mass of injected fuel in order to track the target
293 rotational speed in spite of changes in load torque.

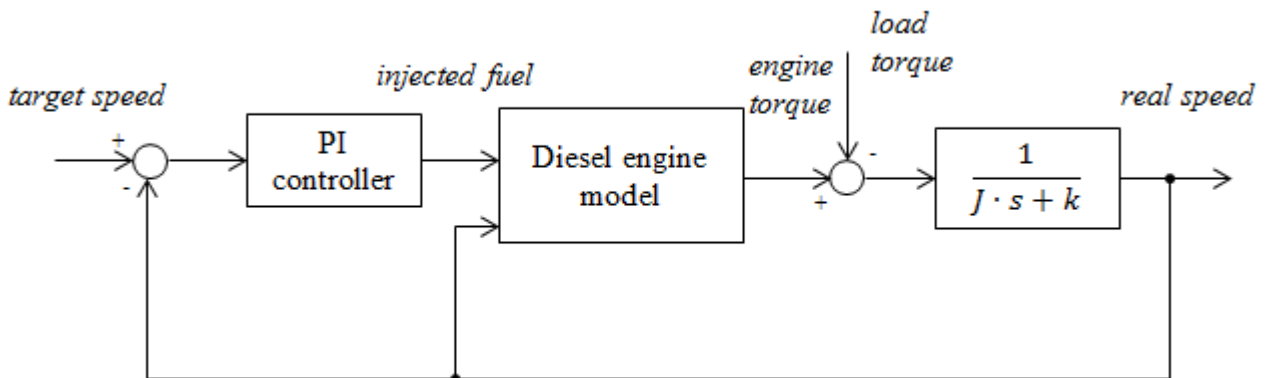


Fig.10. Schematic of the engine-load control.

297 The overall engine model was then identified on the basis of steady-state experimental data from
 298 Yanmar with the aim to obtain the expected values for BSFC and power output for given values of
 299 engine speed and fuel mass flow rate (figs.8 and 9). Parameters a , b and c in eq.(12) were tuned to
 300 obtain the maximum engine torque at 2200r/min corresponding to a start of injection (SOI) of
 301 13degCA, as stated on the engine data sheet. In other operating conditions the SOI has been tuned to
 302 the minimum value corresponding to the maximum output torque. Following the usual tuning
 303 procedures to obtain the maximum efficiency [36], effects of SOI on torque output were estimated by
 304 the model (fig.11) then allowing defining the optimal SOI value (fig.12).

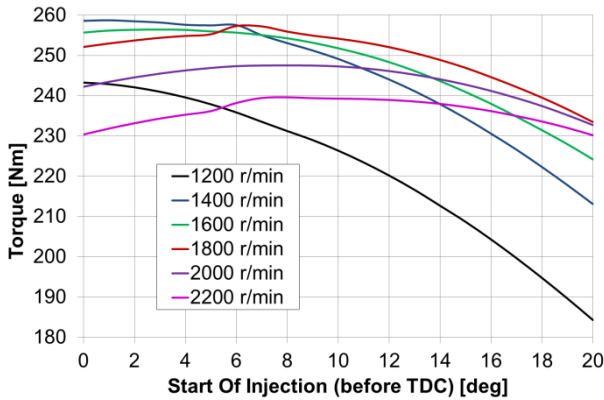


Fig.11. Simulated torque output vs. SOI for different engine speeds.

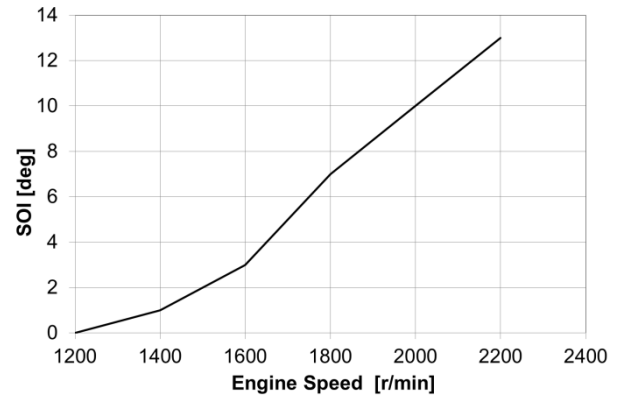


Fig.12. Defined map of SOI [degCA] as a function of rotational speed.

305 The engine model was finally validated by comparing simulated torque characteristic with
 306 experimental data given by the OEM. Results reported in fig.13 show a satisfactory agreement, with
 307 errors below 5% and the overall trend reproduced adequately.

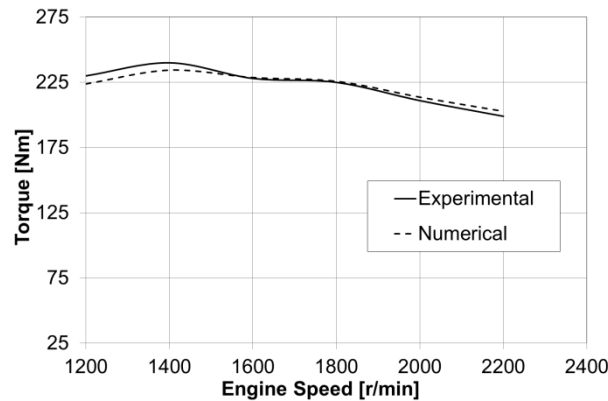


Fig.13. Simulated and experimental engine torque characteristic.

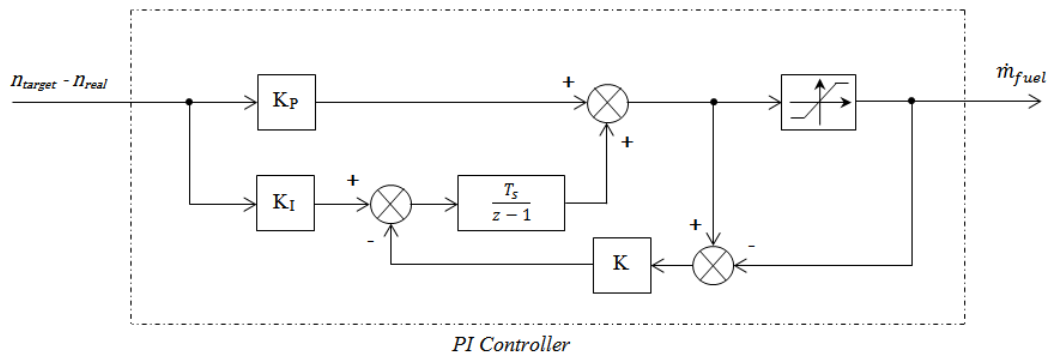


Fig.14. PI Controller Scheme.

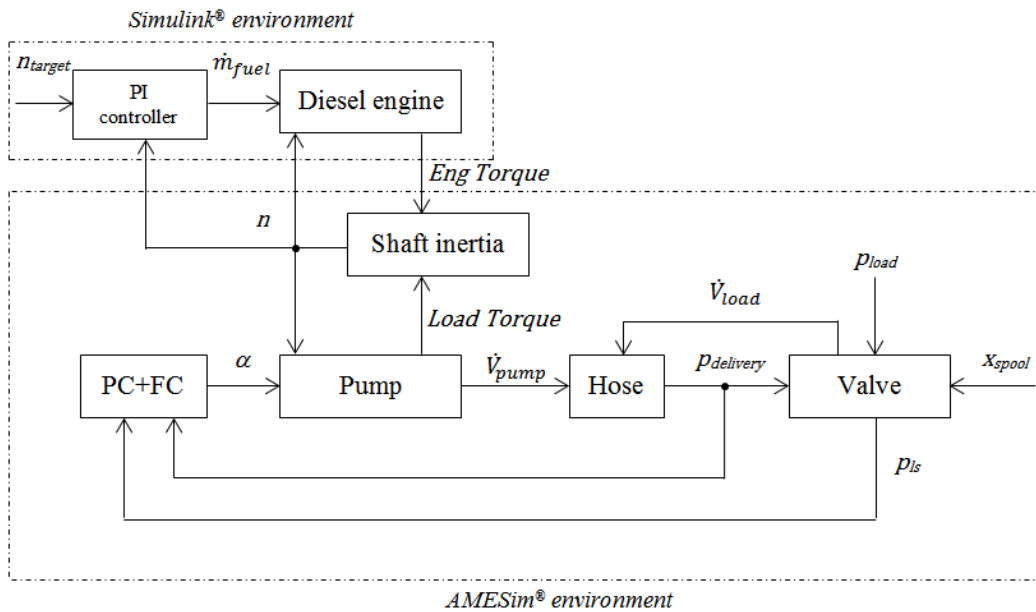
308

309 The engine control strategy has been implemented as a very simple PI controller with saturation and
 310 tracing anti-windup back calculation [38], fig.14, where the proportional gain (K_P), the integral gain
 311 (K_I) and the back tracking gain (K) have been calibrate on the following limitations specified by the
 312 engine OEM:

- 313 • while the load changes from 100% to 0, a maximum engine speed overshoot of 12% of the
 314 rated value (2200r/min) is accepted, maximum steady state error over engine speed is imposed
 315 equal to 6.8% of the rated value;
- 316 • a maximum rise time of 6s is allowed by the OEM.

317 4. Coupling Hydraulic System and Engine models: the comprehensive excavator model.

318 The models of the hydraulic circuit and the internal combustion engine have been properly coupled
 319 together complying with causality to develop a typical excavator system mathematical model [25]. The
 320 kinematic has not been taken into account during this phase, and in order to replicate realistic loads
 321 and flow rates on the valve, the experimental data measured during the operating cycle (described in
 322 section 5) have been imposed to the valve's ports (i.e. p_{load} and X_{spool}). Fig.15 reports the scheme of the
 323 simulated model, where the internal combustion engine and the hydraulic mathematical models are
 324 physically linked taking account of balance of momentum at the engine shaft and of shaft dynamics.
 325 Load torque is evaluated from eq.(7), depending on pump mass flow rate (i.e. on swash plate angular
 326 position α) and delivery pressure, while the engine define an engine torque (Eng Torque) mean value
 327 over the cycle. The approach used for both models does not consider high frequency behaviors,
 328 therefore the overall model is able to take account of low frequency interactions between the hydraulic
 329 system and the engine.

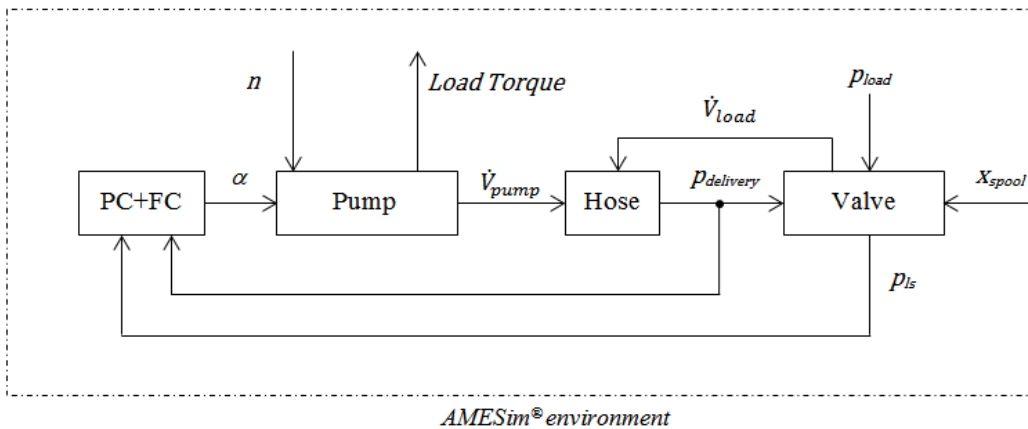


330

331 **Fig.15.** Sketch of the simulation model with internal combustion engine and hydraulic system.

332 In order to evaluate the advantages of having a dynamic model of the engine coupled with the
 333 hydraulic system instead of a constant speed model, during the control algorithm definition procedure,
 334 the simulation model reported in fig.16 have been defined.

335 The experimental data and the simulation results of the two models have been compared in section
 336 5.



337

338 **Fig.16.** Sketch of the simulation model with the hydraulic system only.

339

340 Since engine and hydraulic system models were developed using two different simulation tools (i.e.,
 341 Simulink® and AMESim®), the latter has been reduced to an “S-Function” and imported into
 342 Simulink® environment [40]. Equations of both models were solved using Euler fixed step method
 343 adopting two different time steps, i.e., 2ms for the engine model and about 80ns for the hydraulic
 344 circuit to avoid numerical instabilities which usually arise when solving with a fixed step method a
 345 stiff set of equations. This is due to the faster dynamics of the hydraulic system caused by the high
 346 bulk modulus of the working fluid.

347 With these specifications, the complete model proved to run on a 2.2GHz Quad Core Pentium PC
 348 with 8GB RAM reaching a satisfying ratio of computation time over physical time (always lower than
 349 0.9).

350 **5. Experimental activity and model validation.**

351 In order to validate the proposed mathematical model, a preliminary dedicated experimental activity
352 was carried out on a middle size (9 ton) excavator (fig.17) equipping the engine and the hydraulic
353 circuit previously described. The bucket actuator was instrumented to measure the pressures inside the
354 actuator's chambers during the operated working cycle, while the boom and the arm actuators were not
355 instrumented. Other operating parameters of interest were measured (see tab.2) to assess system
356 response and performance during the testing cycles. Data was acquired with a sample frequency of
357 100Hz to capture properly transient behaviour of the system.

358
359 *Tab.2. Operating parameters measured during the experimental investigation.*

360

<i>Parameter</i>	<i>Sensor</i>
Pump delivery pressure, $p_{delivery}$	Strain gauge
Load Sensing pressure, p_{LS}	Strain gauge
Bucket actuator pressure, p_{load}	Strain gauge
Swash angle, α	LVDT

361



Fig.17. The middle size excavator considered in the experimental activity.

362 The working cycle considered during this working phase involved just the bucket movement.
363 Starting from the fully extended position, the operator acted on the valve control joystick moving the
364 valve spool to completely extend the actuator piston, therefore closing the bucket. Afterward, the
365 actuator piston was moved backward to return the bucket in the initial position and the cycle could be
366 repeated.

367 In order to study the behaviour of the system, with particular reference to the engine, the described
368 working cycle has been carried out for two values of the target engine speed n_{target} , i.e., 1480r/min
369 (case 1) and 1750r/min (case 2).

370 Measured data were compared with theoretical results from the mathematical models described in
371 section 4. Input parameters for the models (see section 4) are the valve spool opening position x_{spool} ,
372 the bucket actuator pressure p_{load} and the engine target velocity n_{target} .

373 In order to show the advantages of having a dynamic model of the internal combustion engine
374 coupled with the dynamic model of the hydraulic system, the experimental measured data were
375 compared with the simulation results obtained with both the model showed in fig.14 (with the engine
376 model) and the model showed in fig. 15 (with the pump rotating at a constant speed, i.e. without the
377 engine model). Figs.18 and 19 show the measured time histories of the spool position x_{spool} for case 1
378 and case 2 respectively. In figs.20 and 21 the experimental time histories of bucket actuator pressures
379 p_{load} for both cases are reported.
380

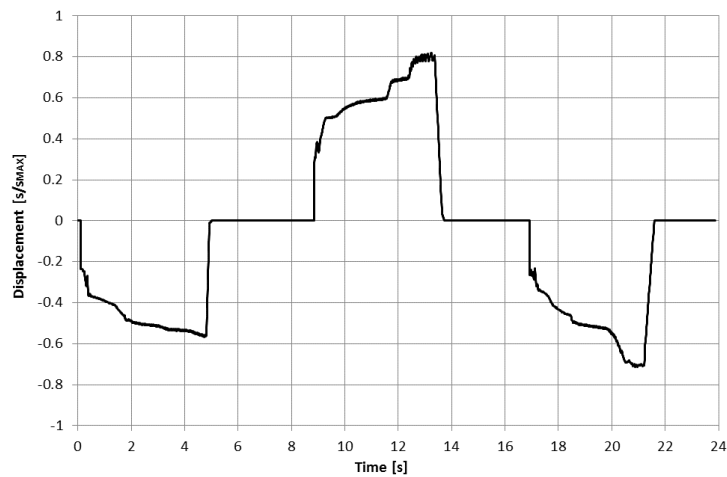


Fig.18. Valve spool opening position x_{spool} measured during the working cycle and used as input for the simulation (case 1).

381

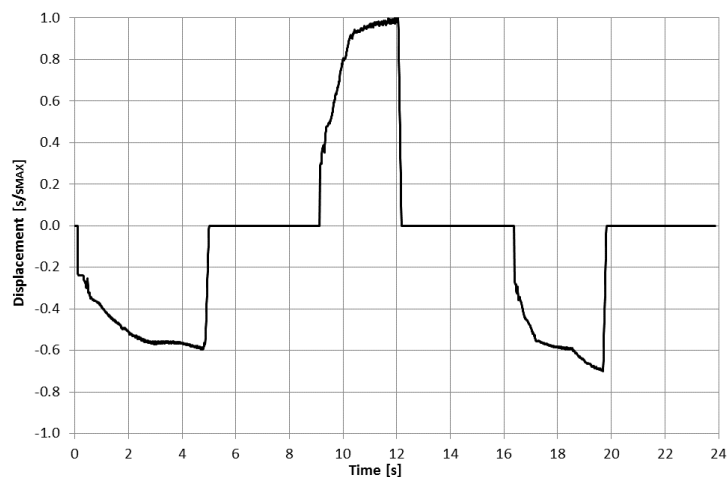


Fig.19. Valve spool opening position x_{spool} measured during the working cycle and used as input for the simulation (case 2).

382

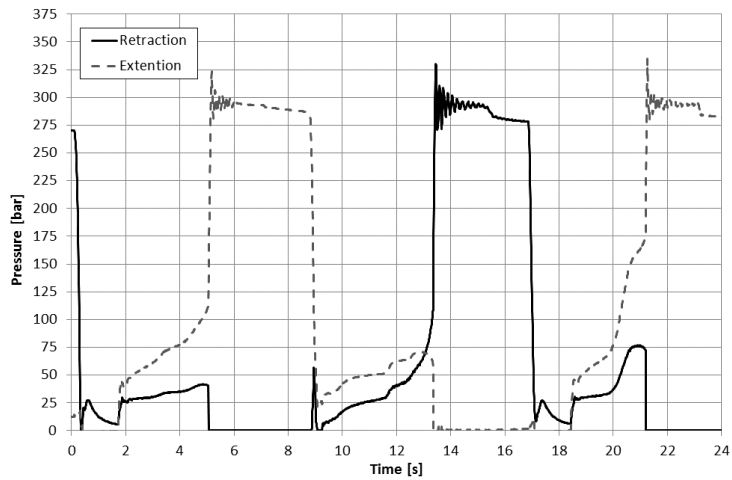


Fig.20. Bucket actuator chambers pressures p_{load} measured during the working cycle and used as input for the simulation (case 1).

383

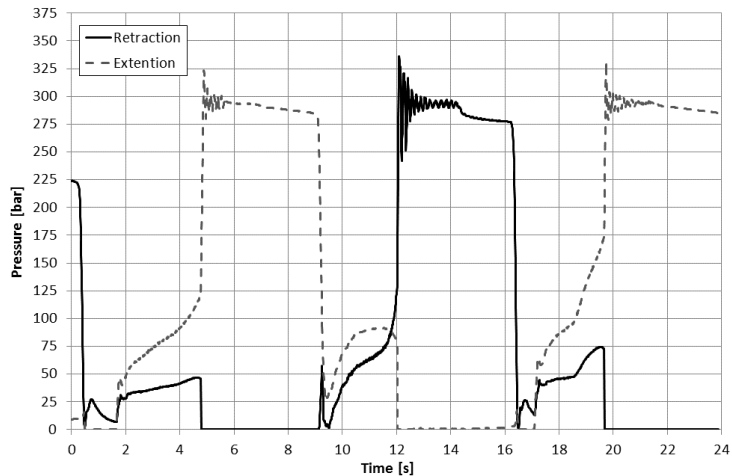


Fig.21. Bucket actuator chambers pressures p_{load} measured during the working cycle and used as input for the simulation (case 2).

384

385 Experimental data and simulation results are compared in figs.22÷24 for a target velocity n_{target}
 386 equal to 1480 r/min (case 1) and in figs.26÷29 for a target velocity n_{target} equal to 1750 r/min (case 2).

387 Both the models were able to estimate p_{LS} changes during considered transients for both target
 388 speed values, as shown in figs.22 and 26. Comparing fig.20 with fig.22 it is evident that the actual
 389 pressure measured in the actuator chamber p_{load} is slightly different from the actual pressure p_{LS} : this
 390 pressure loss is due to hydraulic line resistance (considered in the model of the hydraulic circuit). It
 391 should be noted that the valve defines the pressure p_{LS} only when the main spool is open, and therefore
 392 when the operator closes the valve orifice p_{LS} drops nearly to zero. The same considerations can be
 393 recalled when comparing figs.21 and 26. Anyway, results reported in figs.22 and 26 show the
 394 capabilities of the proposed mathematical model to reproduce the real regulator behaviour, being the
 395 curves almost overlapped.

396 Small differences can be also pointed out with reference to pump delivery pressure $p_{delivery}$, as
 397 shown in figs.23 and 27, for the studied cases.

398 Observing figs. 24 and 28, where the comparison between experimental and simulation results for
 399 the swash plate angle position α are reported, it is possible to notice the advantages on having a

400 dynamic model of the internal combustion engine coupled with the hydraulic system, instead of simply
401 setting a constant velocity source for the pump. In fact when the operator opens or closes quickly the
402 valve's main spool, a variation on the shaft speed occurs, as reported in figs. 25 and 29. In these
403 situations the pump's regulator defines a new swash plate position in order to meet the hydraulic
404 system pressure demand while the engine PI controller acts in order to keep the shaft speed at the
405 reference value.

406 The mathematical model with the engine shows simulated engine speed transients trends very
407 similar to experimental data, figs. 25 and 29, and better results are showed for the swash plate angle
408 position too, compared with the mathematical model without the engine dynamic model.

409

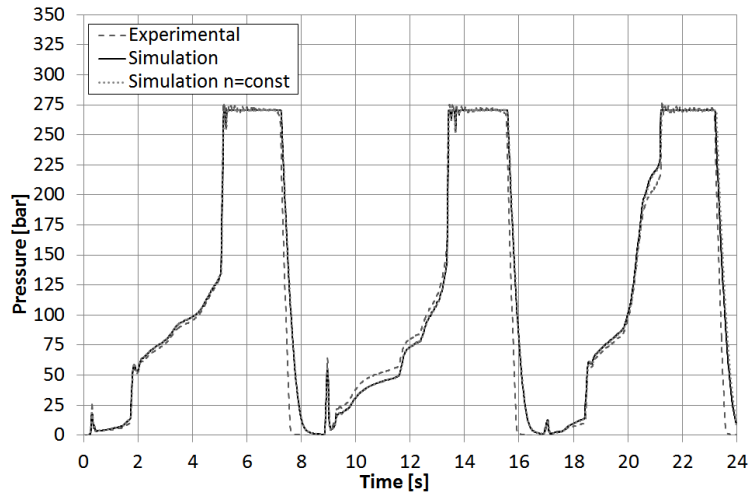


Fig.22. Measured and calculated transients for p_{LS} (case 1).

410

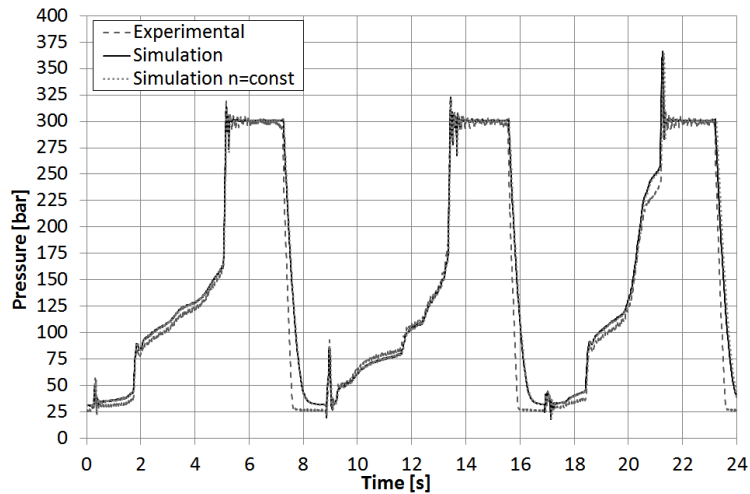


Fig.23. Measured and calculated transients for $p_{delivery}$ (case 1).

411

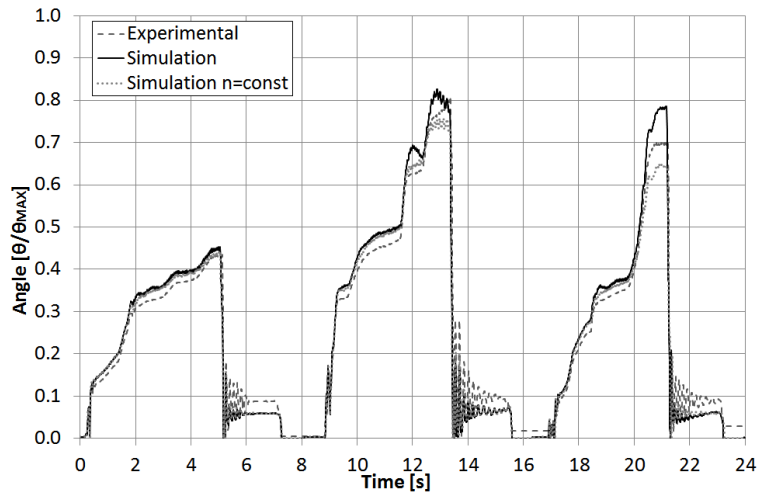


Fig.24. Measured and calculated transients for swash plate angle α (case 1).

412

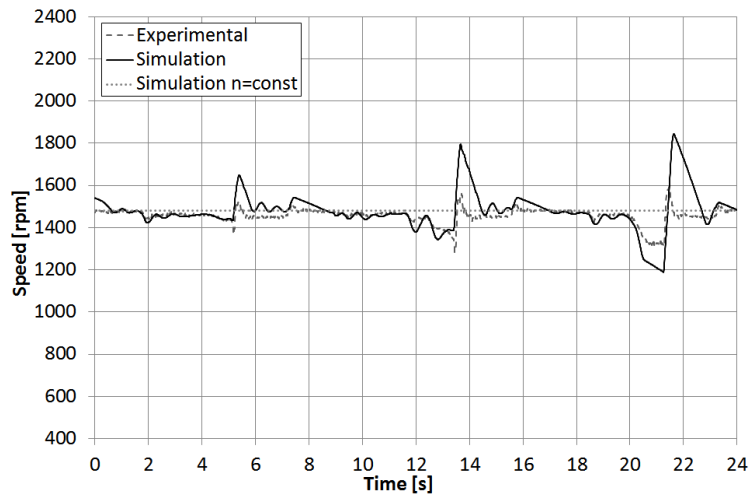


Fig.25. Measured and calculated transients for engine speed (case 1).

413

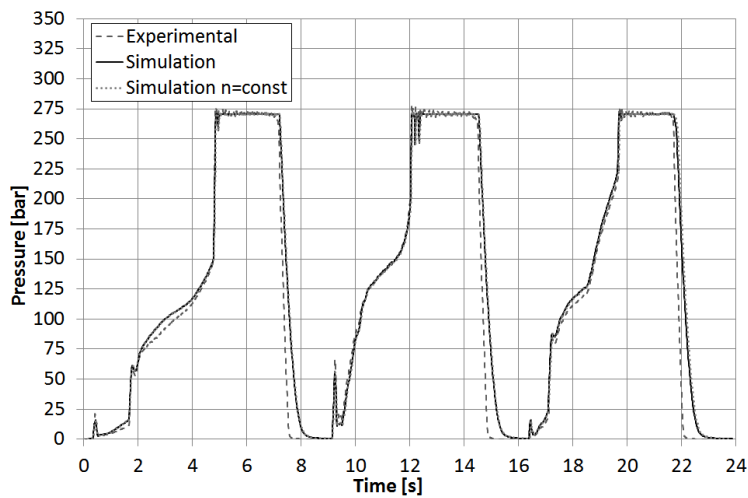


Fig.26. Measured and calculated transients for p_{LS} (case 2).

414

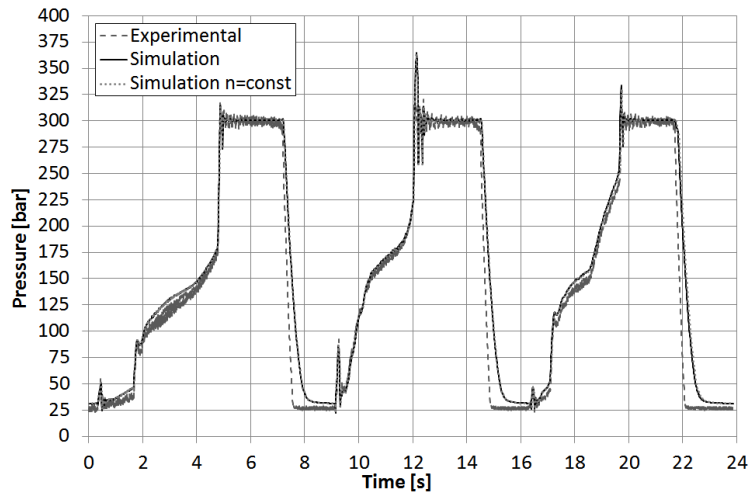


Fig.27. Measured and calculated transients for $p_{delivery}$ (case 2).

415

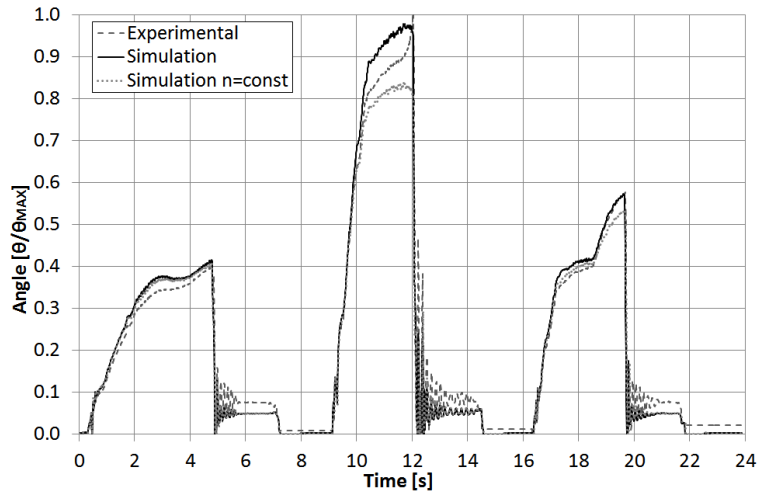


Fig.28. Measured and calculated transients for swash plate angle α (case 2).

416

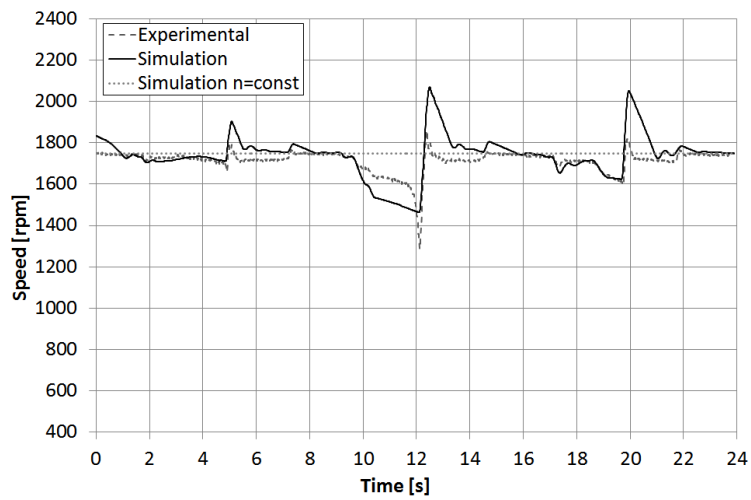


Fig.29. Measured and calculated transients for engine speed (case 2).

417

418 **6. Conclusions**

419 The paper is primarily aimed at the development of fast control-oriented simulation models of a typical
420 mobile machinery, where hydraulic systems are coupled to internal combustion engines as prime
421 movers. Hydraulic system model was built up within the AMESim® environment while the engine
422 model was created in Simulink®. Results reported in the paper show how mathematical models of
423 complex systems can be built up through co-simulation, i.e., merging proper sub-models even if from
424 different modelling environment. Major difficulties that had to be solved in the presented work were
425 related to the definition of integration time steps of merged sub-models, since they had to be chosen
426 taking account of their numerical “stiffness” (significantly different when dealing with gaseous or
427 liquid fluids). Notwithstanding the use of different time steps, the comprehensive model proved to run
428 on a current PC faster than Real-Time. The comparison of calculated results with experimental data
429 from a dedicated investigation showed that the model is able to predict system behaviour during fast
430 transients with errors lower than 10% (with reference to pressures, engine speed and swash plate
431 angle). The methodology adopted to formulate the model of the excavator can be used for control-
432 oriented applications as a mathematical tool in the three typical levels of the optimization process, i.e.:
433 definition of the optimal configuration of the system, since modularity of the model allows to change
434 easily the layout of the system to investigate how it affects the overall behaviour; selection of the best
435 size of all components, for the reason that all sub-models are physical-based and therefore can be
436 easily modified; design of an optimized control strategy for the system through an easy link of the
437 system model with the control unit(s) model(s), since the architecture of the overall model allows its
438 implementation in MiL, SiL and HiL system widely used to define, test and optimize Electronic
439 Control Units. The main advantage of the proposed co-simulation approach based on matching models
440 from different environments is the use of the same tools to comply with each one of the mentioned
441 level thus leading to a reduction of development time and costs and to a better understanding of the
442 behaviour of the whole system. To this extent improvements considered for further development of the
443 methodology will involve the application of the proposed modelling techniques to enhanced layouts
444 (e.g., hybrid systems with hydraulic storage) and the implementation of the models in a real SiL/HiL
445 system.

446 **Acknowledgments**

447 The authors would like to acknowledge the active support of this research by Casappa S.p.A.,
448 Parma and Walvoil S.P.A (ITALY).

449 **References**

- 450 [1] T.Costlow, “Making sense of hybrids”, SAE Off-Highway Engineering, april 2014.
451 [2] M.Inderelst, S.Losse, S.Sigro, H.Murrenhoff, “Energy efficient system layout for work
452 hydraulics of excavators.”, 12th Scandinavian International Conference on Fluid Power, 2011,
453 Tampere, Finland. ISBN 978-952-15-2520-9.
454 [3] G.Altare, D.Padovani, N.Nervegna, “A Commercial Excavator: Analysis, Modelling and
455 Simulation of the Hydraulic Circuit.”, SAE Technical Paper 2012-01-2040, 2012,
456 doi:10.4271/2012-01-2040.
457 [4] M.Erkkilä, F.Bauer, D.Feld, “Universal Energy Storage and Recovery System – A Novel
458 Approach for Hydraulic Hybrid”, The 13th Scandinavian Int.Conf.on Fluid Power, SICFP2013,
459 2013, Linköping, Sweden.

- 460 [5] K.Renz, K.-H. Vogl, M.Brand, “Hydraulic Energy Storage^[1] for Hydrostatic Travel Drives”,
461 ATZ Magazine, Special edition on Energy Storage, pp.62-70.
- 462 [6] M.Conrad, “Hydraulic Hybrid Vehicle Technologies”, Clean Technologies Forum, Sacramento,
463 USA, 2008.
- 464 [7] S.Hui, Y.Lifu, J.Junqing, L.Yanling, “Control strategy of hydraulic/electric synergy system in
465 heavy hybrid vehicles”, Energy Conversion and Management, vol.52, 2011, pp. 668–674.
- 466 [8] D.Feng, D.Huang, D.Li, “Stochastic Model Predictive Energy Management for Series Hydraulic
467 Hybrid Vehicle”, Proceedings of the 2011 IEEE^[1] International Conference on Mechatronics and
468 Automation, Beijing, China, 2011.
- 469 [9] T.H.Ho, K.K.Ahn, “Design and control of a closed-loop hydraulic energy-regenerative system”,
470 Automation in Construction, vol.22, 2012, pp.444–458.
- 471 [10] B.Wu, C.-C.Lin, Z.Filipi, H.Peng, D.Assanis, “Optimal Power Management for a Hydraulic
472 Hybrid Delivery Truck”, Vehicle System Dynamics, 2004, Vol.42, No.1–2.
- 473 [11] Z.Filipi, Y.J.Kim, “Hydraulic Hybrid Propulsion for Heavy Vehicles: Combining the Simulation
474 and Engine-In-the-Loop Techniques to Maximize the Fuel Economy and Emission Benefits”, Oil
475 & Gas Science and Technology–Rev.IFP, Vol.65 (2010), No.1, pp.155-178,
476 doi:10.2516/ogst/2009024.
- 477 [12] F.A.Bender, M.Kaszynski, O.Sawodny, “Location-Based Energy Management Optimization for
478 Hybrid Hydraulic Vehicles”, 2013 American Control Conference (ACC), Washington, USA,
479 2013.
- 480 [13] K.Patil, S.K.Molla, T.Schulze, “Hybrid Vehicle Model Development using ASM-AMESim-
481 Simscape Co-Simulation for Real-Time HIL Applications”, SAE paper no. 2012-01-0932, 2012,
482 doi:10.4271/2012-01-0932.
- 483 [14] I.Cosadia, J.J.Silvestri, I.Papadimitriou, D.Maroteaux, P.Obernesser, “Traversing the V-Cycle
484 with a Single Simulation - Application to the Renault 1.5 dCi Passenger Car Diesel Engine”,
485 SAE technical paper no.2013-01-1120.
- 486 [15] P.Casoli, A.Anthony, “Gray box modeling of an excavator’s variable displacement hydraulic
487 pump for fast simulation of excavation cycle”, Control Engineering Practice, vol.21, pp.483-494,
488 Elsevier, 2013, <http://dx.doi.org/10.1016/j.conengprac.2012.11.011>.
- 489 [16] A.Gambarotta, G.Lucchetti, I.Vaja, “Real-time Modelling of Transient Operation of
490 Turbocharged Diesel Engines.” 2011, Proc. I.Mech.E., Part D: Journal of Automobile
491 Engineering, Vol. 225, ISSN 0954-4070.
- 492 [17] P.Casoli, A.Gambarotta, N.Pompini, U.Caiazzo, E.Lanfranco, A.Palmisano, “Development and
493 validation of a “crank-angle” model of an automotive turbocharged Engine for HiL
494 Applications”, Energy Procedia, Elsevier, 2014, doi: 10.1016/j.egypro.2014.01.089.
- 495 [18] P.Casoli, A.Anthony, L.Riccò, “Modeling of an Excavator System – Load sensing flow sharing
496 valve model”, SAE 2012 Commercial Vehicle Engineering Congress, Rosemont, Illinois, USA,
497 2012, doi:10.4271/2012-01-2042.
- 498 [19] D.McCloy, H.M.Martin, “The control of Fluid Power”, Hellis Horwood Limited, London, 1973,
499 ISBN 0-85312-135-4.
- 500 [20] P.Casoli, A.Vacca, G.Franzoni, G.L.Berta, “Modeling of fluid properties in hydraulic positive
501 displacement machines.”, Elsevier, Simulation Modeling Practice and Theory, vol.14, Issue 8,
502 November 2006, pp.1059-1072 ISSN: 1569-190X. doi:10.1016/j.simpat.2006.09.006.
- 503 [21] M.Zecchi, M.Ivantysynova, “Cylinder Block/Valve Plate Interface – a Novel Approach to
504 Predict Thermal Surface”, 8th International Fluid Power Conference, Dresden, March 26-28,
505 2012.
- 506 [22] M.Borghini, E.Specchia, B.Zardin, “Numerical Analysis of the Dynamic Behaviour of Axial
507 Piston Pumps and Motors Slipper Bearings”, SAE International Journal of passenger cars -
508 Mechanical System, vol.2, pp.1285-1302, ISSN: 1946-3995, 2009.
- 509 [23] M.Pelosi and M.Ivantysynova, “A new Fluid-Structure Interaction Model for the Slipper-Swash
510 Plate Interface.”, Proc.5th FPNI Ph.D. Symposium, Cracow, Poland, pp.219-236, 2008.
- 511 [24] P. Casoli, A. Gambarotta, N. Pompini, L. Riccò (2014). “Development and application of co-
512 simulation and control-oriented modeling in the improvement of performance and energy saving

- of mobile machinery”, Energy Procedia, Volume 45, 2014, Pages 849–858. Elsevier. <http://dx.doi.org/10.1016/j.egypro.2014.01.090>. Codice Scopus: 2-s2.0-84893640233.
- [25] L.Guzzella, C.H.Onder – “Introduction to Modelling and Control of Internal Combustion Engine Systems.” – Springer-Verlag, Berlin, 2010.
- [26] L.Guzzella, A.Amstutz, “Control of Diesel engines”, IEEE Trans.on Control Systems Tech., vol.18 (5), 1998.
- [27] N.Watson, M.S.Janota – “Turbocharging the internal combustion engine” – John Wiley and Sons, 1982.
- [28] J.B.Heywood – “Internal Combustion Engines Fundamentals” – McGraw-Hill, New York, 1988.
- [29] O.E.Doebelin, “System Dynamics: modelling, analysis, simulation, design”, Marcel Dekker Ed., New York, 1998.
- [30] D.Anguina, P.Casoli, M.Canova, A.Gambarotta, F.Riviuccio – “A learning-machine based method for the simulation of combustion process in automotive I.C.Engines” – Spring Conference of the I.C.Engines Division of the ASME, paper no.ICES2003-682, Salzburg, 2003.
- [31] J.Sun, I.Kolmanovsky, J.A.Cook, J.H.Buckland, “Modeling and Control of Automotive Powertrain Systems: a Tutorial”, American Control Conference, Portland, June 2005.
- [32] M.Canova, P.Fiorani, A.Gambarotta, M.Tonetti – “A real-time model of a small turbocharged Multijet Diesel engine: application and validation.” – Proc.7th SAE-NA Int.Conf.on Engines for Automobiles, SAE paper no.2005-24-65, Capri, 2005.
- [33] P.Fiorani, A.Gambarotta, E.Lanfranco, M.Tonetti – “A real-time model for the simulation of transient behaviour of automotive Diesel engines.” – Proc.ATI/SAE Congress “The sustainable mobility challenge”, SAE paper no.2006-01-3007, Perugia, 2006.
- [34] A.Gambarotta, G.Lucchetti, M.Taburri, I.Vaja – “Mean Value Modeling of intake and exhaust systems of automotive engines: models identification and related errors” – 10th Stuttgart International Symposium on Automotive and Engine Technologies, Stuttgart, 2010.
- [35] A.Gambarotta, G.Lucchetti, I.Vaja, “Real-time Modelling of Transient Operation of Turbocharged Diesel Engines”, Proc. I.Mech.E., Part D: J. Automobile Engineering, Vol. 225, 2011, ISSN 0954-4070, DOI:10.1177/0954407011408943.
- [36] Robert Bosch GmbH, “Diesel engine management”, John Wiley & Sons, 2006.
- [37] LMS Imagine, AMESim® Reference manual 2011.
- [38] M.Tharayil and A.Alleyne. A generalized pid error governing scheme for SMART/SBLI control. IEEE American Control Conference, 1: 346-351, May 2002
- [39] LMS Imagine.Lab AMESim. Activity Index REV13 User’s Guide
- [40] Louca L.S. “Modal analysis reduction of multi-body systems with generic damping”, Journal of Computational Science 5 (2014) 415–426. doi:10.1016/j.jocs.2013.08.008].

548 Definitions

549	<i>m</i>	mass
550	<i>n</i>	rotational speed (in [r/min])
551	<i>p</i>	pressure
552	<i>t</i>	time
553	<i>T</i>	torque
554	<i>V</i>	volume
555	ρ	fluid density
556	η	efficiency

557 Subscripts

558	<i>d</i>	displacement
559	<i>hm</i>	hydro-mechanical
560	<i>v</i>	volumetric
561		

562 Acronyms

563	F&E	Filling-and-Emptying
564	HHS	Hydraulic Hybrid System
565	ICE	Internal Combustion Engine
566	LS	Load-Sensing
567	MVM	Mean Value Model
568	QSF	Quasi Steady Flow

